Reports

Active Polar Region on the Nucleus of Comet Halley

H. J. Reitsema, W. A. Delamere, F. L. Whipple

The images of the nucleus of comet Halley returned by the Giotto spacecraft reveal a number of active regions on the surface, one of which is near the expected location of the rotation pole. This feature is larger and brighter than other source regions, suggesting that the mechanism that drives this source is also different. At this active region near the rotation pole, the sun was circumpolar for a significant portion of the solar encounter. Continuous insolation heated the nucleus to greater depths than in other areas, producing the broad, active polar region.

Images and other data returned by the European Giotto spacecraft (*1*) and the two Soviet Vega spacecraft (*2*), together with intensive observations from the ground-based International Halley Watch and several space observatories, have been used to develop a consistent picture of the nucleus of comet Halley. The nucleus is roughly elliptical in shape, with dimensions of about 16 by 8 by 8 km (*3*). The dirty snowball model of Whipple (*4*) was largely confirmed, and the existence of a dark surface mantle has been established. This mantle thermally insulates the icy interior of the comet and limits dust jet activity to areas on the nucleus where the mantle is thin or nonexistent or has been disturbed.

Several source regions were identified in the Giotto images (*5, 6*), covering about 10% of the observed surface. One of these is a very bright, broad region associated with a strong dust feature seen in the coma. Because this feature is located near the sunlit rotation pole, it received insolation for many rotation periods before the Giotto encounter. Its large extent and brightness may result from the continuous thermal input.

After a number of studies of ground-based data (*7–11*), Pioneer Venus spacecraft observations (*12*), and spacecraft images (*2, 13, 14*), there remains considerable uncertainty regarding the spin period and orientation. Periods of both 2.2 and 7.4 days are evident in the data sets. Smith *et al.* (*14*) used profiles of the nucleus determined from the spacecraft images to argue that the spin period is 2.2 days, which we adopt here. The corresponding rotation axis points toward right ascension $\alpha = 50°$ and declination $\delta = -40°$ in 1950 celestial coordinates. The 7.4-day period seen in coma activity has been attributed to nutation (*15*). The best fit to the three spacecraft encounter views gives an axis that is located in the Giotto images at 60° toward ecliptic south from the sun direction and 13° into the plane of the images, as shown in Fig. 1 (*16*). The sunlit pole is located just beyond the visible limb in the Giotto images. The obliquity of the axis is about 25°, giving rise to seasonal variations in the solar illumination of the surface (*17*).

The images of the nucleus obtained with the Halley Multicolour Camera (HMC) on Giotto have been used to determine the limb of the nucleus as seen from the spacecraft (*3*), which may then be used to obtain estimates of the inertial axes of the body. The nucleus profile is shown in Fig. 2, which also indicates the location of the minimum-first-moment "center of gravity" (CG) of the profile. This profile and CG were used to determine the orientation of the principal axes of inertia, also shown in Fig. 2. Because there is little information in the images regarding the line-of-sight dimensions, the limb of the nucleus was taken as the outer boundary of a half-figure of revolution of uniform density. The axis that gave the minimum moment of inertia was taken as the projection of the major body axis. The circular profile seen by Vega 1 shows that the orthogonal cross section is nearly circular; thus the nucleus shape can be approximated by an elongated ellipsoid with axial ratios 1:1:2. The long axis of the nucleus must be nearly coincident with the projection of the long axis of the profile, which is 34° toward ecliptic north from the sun direction. With this spin axis, the nucleus is spinning about its maximum moment of inertia (*18*). There is little evidence for large nutation amplitudes.

The intermediate and maximum axes of inertia lie in a plane perpendicular to the long axis and intersect the image plane at a 90° angle to the long axis, as shown in Fig. 2. Studies of the correlation of Vega and Giotto images (*13, 14*) have indicated that the long axis lies at an angle of roughly 30° out of the plane of the images, with the smaller end lying closer to the spacecraft. Figure 1 shows the configuration of the axes relative to an ellipsoid with axial ratios 1:1:2. The projection of the axis of maximum inertia lies on a narrow ellipse with opening angle of 30°, whose long axis is perpendicular to the long body axis. The angular momentum vector should lie in the plane of this ellipse.

The spin axis determined from the spacecraft images is indicated in Fig. 1. The pole from which the rotation appears counterclockwise is labeled "N" (*19*). This north pole is located within the region of highest dust activity, establishing the association of the unique properties of the source region with the continuous circumpolar insolation.

There remains considerable possible error in the determination of the axes. The axis determined from the three spacecraft encounters may contain errors because the profile of the nucleus is not well defined in the Vega 1 images, and only the terminator and sunlit limb (not the dark limb) are visible in the Vega 2 data. Errors in the determination of axes of inertia from the single Giotto profile may result from the assumption of uniform density and from the fact that the Giotto images give only a two-dimensional view.

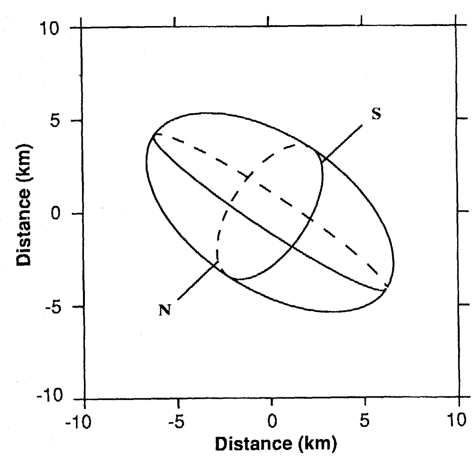

Fig. 1. Orientation of the nucleus ellipsoid relative to the rotation axis. The nucleus is represented by an ellipsoid with axial ratios 1:1:2, and the rotation axis determined from spacecraft images is indicated. The upper end of the long body axis is tipped toward the camera by about 30°, rotating away from the camera (*16*). The convention for identifying rotation poles gives, in the case of Halley, the north rotation pole oriented toward the ecliptic southern hemisphere. Regions near the north rotation pole were continuously illuminated by sunlight at the time of the spacecraft encounters.

H. J. Reitsema and W. A. Delamere, Ball Aerospace Systems Division, Boulder, CO 80306.
F. L. Whipple, Smithsonian Astrophysical Observatory, Cambridge, MA 02138.

The unique bright region near the rotation pole appears to be the source of the dominant dust emission in the coma. Figure 3, taken with the HMC on the Giotto spacecraft, shows the active region near the north rotation pole of the nucleus. The visible portion of the polar region covers a surface area of about 4 km^2 near the center of the sunlit limb and probably extends into the far hemisphere. The limb of the nucleus is evident as a step decrease in brightness toward the left, indicating that the bright patch is caused by surface brightness rather than by an overlying dust cloud, which would have a gradual decrease. The bright area has an albedo of about 6% (*16*); it is about 1.5 times as bright as the surrounding surface, suggesting that the dark surface mantle has been removed or modified in this area.

This polar region is clearly associated with a broad dust emission feature but is distinctly different from the source regions for the dust jets associated with the bright tip of the nucleus, which are also quite bright but are much smaller, having dimensions of no more than 1 to 2 km. Although the apparent surface brightness of this feature is not as great as for the active regions near the northern tip, images of the coma taken from Giotto at greater distances reveal that most of the dust emission is directed into the (ecliptic) southern hemisphere (*5*). Figure 4 shows an image taken about 30 minutes before flyby from a range of 104,000 km. The strong asymmetry of the dust emission relative to the direction of the sun may be caused by the emission from the polar region, presumably including dust from the extension of the polar region on the far side of the nucleus.

The existence of the active circumpolar region implies that there would be significant dust emission from that region throughout a cometary season. The Vega 2 pictures, taken 8 days earlier, have a clear asymmetry in dust emission toward the south. Sagdeev *et al.* (*20*) have analyzed Vega 2 pictures from a range of phase angles to determine the points of origin for the coma dust. Although this analysis used a sun-oriented spherical coordinate system that ignored the shape of the nucleus, the derived source regions were predominantly in the (ecliptic) southern direction and are generally consistent with the polar active region source. Ground-based observations of the inner coma also show a southern asymmetry in dust production (*21*); the asymmetry is not significant at larger distances.

The mantle thermally isolates most of the surface from the diurnal heat wave, restricting activity to regions where the mantle has been disturbed or removed. The obliquity of the comet's spin axis causes the sun to be circumpolar from latitudes near the sunward pole, and, except for short periods near the equinoxes, the insolation in the polar region is not modulated in a 2.2-day diurnal cycle. Even though the solar elevation angle is low, the continuous solar input will cause the mantle temperature to rise. The thermal wave will extend to greater depths in the mantle at the polar region and may reach undisturbed ice and dust in the underlying nucleus. The resulting heating of the nucleus produces increased gas flow that can entrain and remove the overlying dust mantle.

Different regions of the comet surface can be expected to have differing thicknesses of mantle, which will lead to inhomogeneities in the response of the surface to solar radiation. The thermal inertia of the mantle and its thickness are the controlling parameters in modeling the transfer of heat from the surface to the underlying undisturbed nucleus. In areas with little or no mantle, activity will begin near sunrise and end shortly after sunset, whereas activity may turn on and off more slowly in regions with higher thermal inertia in the mantle. In areas where the time constant for turn-on is greater than half the 2.2-day rotation period, no activity will develop except near the polar region, where continuous solar input can penetrate the mantle and produce activity.

The activity at the north rotation pole would begin some time after the "spring" equinox, which occurred near perihelion (*17*). Before perihelion, the south rotation pole would have had continuous sunlight. Thus, different polar source regions would have been involved in both a continuous polar dust emission and any nutation-modulated sources near the sunlit pole. Nearer to perihelion, neither pole would receive significant solar input, the dust emission would be dominated by subsolar sources, and all sources would be modulated at the diurnal rate.

The observations of the polar region in the Giotto images give strong evidence that the mantle has been substantially eroded at the solar circumpolar region. The brightness of the surface is a result of the removal of much of the dark material, and the resulting

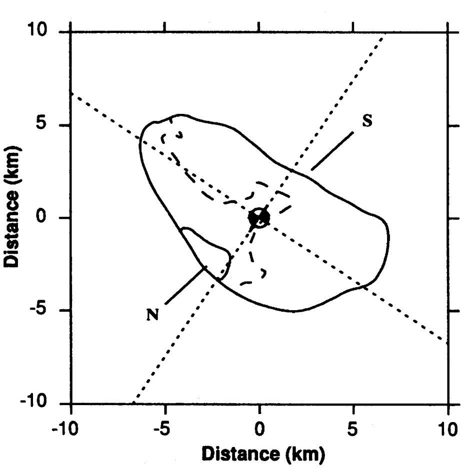

Fig. 2. Profile of the nucleus as seen by Giotto (*3*), showing morning terminator (dashed line) and the approximate boundary of the polar region (solid line inside the nucleus profile). Dotted lines show the major and minor axes of the profile, and the center of gravity is indicated. The rotation axis from Fig. 1 is shown here relative to the profile axes and polar region.

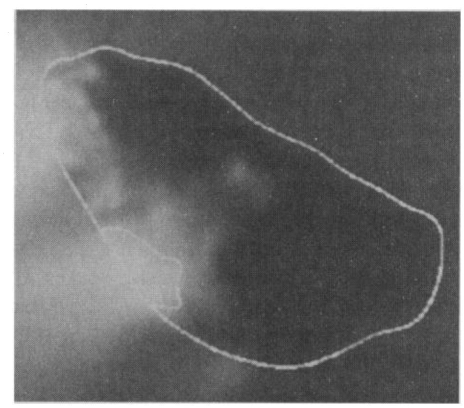

Fig. 3. North polar region on the nucleus. The area is brighter than the surrounding surface and broader than the active region visible near the subsolar point at upper left. The polar region is the source for the major dust feature seen by spacecraft and ground-based observers at the time of encounter. The orientation for all figures is the same, with ecliptic north up and the sun toward the left, 17° below the image plane. White lines mark the boundaries of the profile and the polar region.

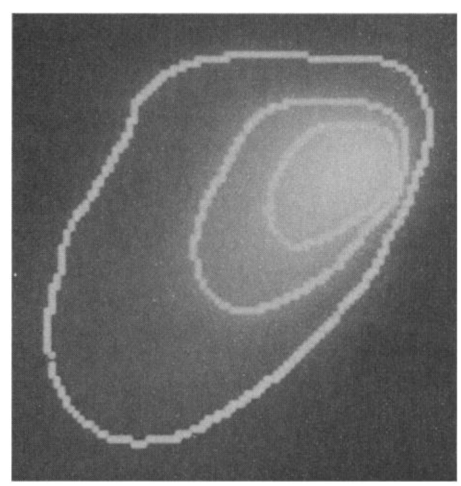

Fig. 4. Image of Halley from a range of 104,000 km. Two isophotal contours are superimposed; these indicate that the strongest dust emission is not in the sunward direction but rather is directed toward the south. Dust ejected from the polar region is the dominant jet seen from this distance. Approximately one-third of the dust in the coma originates in the polar region (*5*).

exposed nucleus is very active in response to the direct insolation. Because the activity will continue for many rotations, the polar region is expected to lose more material than other regions. Evidence for such erosion may be found in the depressed "broad central plain" described by Keller *et al.* (*16*) (although the limb profile shows no depression at the region of activity).

The enhanced activity at the polar region is likely to extend over the entire solar circumpolar area, with the rotation pole lying at the center of the active area. Because Giotto obtained images only from the approach direction, there are no data on the extent of the polar active zone on the other face of the nucleus. However, comparison of the observed active region with the expected circular shape of the active polar zone suggests that the pole lies near the limb of the nucleus, consistent with other values for the rotation axis. Any nutation will affect the insolation at the solar circumpolar regions, and the 7.4-day modulation of the coma activity may be related to the effects of nutation, causing the position of a source region to alternate between inside and outside the solar circumpolar zone.

REFERENCES AND NOTES

1. R. Reinhard, *Nature* **321**, 313 (1986).
2. R. Z. Sagdeev *et al.*, *ibid.*, p. 262.
3. H. J. Reitsema *et al.*, in *Proceedings of the 20th ESLAB Symposium on the Exploration of Halley's Comet*, B. Battrick, E. J. Rolfe, R. Reinhard, Eds. (Publication ESA SP-250, European Space Agency, Paris, 1986), pp. 351–354.
4. F. L. Whipple, *Astrophys. J.* **111**, 779 (1950).
5. H. U. Keller *et al.*, *Nature* **321**, 320 (1986).
6. H. J. Reitsema, W. A. Delamere, F. L. Whipple, in *Proceedings of the Symposium on the Diversity and Similarity of Comets*, E. J. Rolfe and B. Battrick, Eds. (Publication ESA SP-278, European Space Agency, Paris, 1986), pp. 455–459.
7. Z. Sekanina and S. M. Larson, *Astron. J.* **89**, 1408 (1984).
8. ——, *ibid.* **92**, 462 (1986).
9. M. J. S. Belton, P. Wehinger, S. Wychoff, H. Spinrad, in *Proceedings of the 20th ESLAB Symposium on the Exploration of Halley's Comet*, B. Battrick, E. J. Rolfe, R. Reinhard, Eds. (Publication ESA SP-250, European Space Agency, Paris, 1986), pp. 599–603.
10. R. L. Mills and D. G. Schleicher, *Nature* **324**, 646 (1986).
11. M. C. Festou *et al.*, *Astron. Astrophys.* **187**, 575 (1987).
12. A. I. F. Stewart, *ibid.*, p. 369.
13. K. Wilhelm, *Nature* **327**, 27 (1987).
14. B. A. Smith, S. M. Larson, K. Szegö, R. Z. Sagdeev, *ibid.*, **326**, 573 (1987).
15. Z. Sekanina, *ibid.* **325**, 326 (1987).
16. H. U. Keller *et al.*, *Astron. Astrophys.* **187**, 807 (1987).
17. P. R. Weismann, *ibid.*, p. 873.
18. K. Wilhelm *et al.*, in *Proceedings of the 20th ESLAB Symposium on the Exploration of Halley's Comet*, B. Battrick, E. J. Rolfe, R. Reinhard, Eds. (Publication ESA SP-250, European Space Agency, Paris, 1986), pp. 367–369.
19. This conventional definition of the rotation pole gives, for comet Halley, the north rotation pole oriented toward the ecliptic southern hemisphere. We use the ecliptic designations for cardinal directions.
20. R. Z. Sagdeev *et al.*, *Astron. Astrophys.* **187**, 835 (1987).
21. S. M. Larson, Z. Sekanina, D. Levy, S. Tapia, M. Senay, *ibid.*, p. 639.

22. We thank the Giotto and HMC teams, who were responsible for the success of the mission, and our colleagues on the HMC and Vega imaging teams for their cooperation in sharing data and results. Supported by NASA grants NASW-3573 and NSG-7082.

23 May 1988; accepted 18 October 1988

A Relation to Describe Rate-Dependent Material Failure

BARRY VOIGHT

The simple relation $\dot{\Omega}^{-\alpha}\ddot{\Omega} - A = 0$, where Ω is a measurable quantity such as strain and A and α are empirical constants, describes the behavior of materials in terminal stages of failure under conditions of approximately constant stress and temperature. Applicable to metals and alloys, ice, concrete, polymers, rock, and soil, the relation may be extended to conditions of variable and multiaxial stress and may be used to predict time to failure.

The prediction of deformation and failure of materials from fundamental relations that are based on physically observable internal parameters (such as vacancies, crystalline structure, dislocation structure, and microcracks) can rarely be directly or easily accomplished. In practice, it is therefore necessary to consider empirical propositions, some of which nevertheless have striking if incompletely understood generality. Such a proposition for the terminal stages of rate-dependent material failure is

$$\dot{\Omega}^{-\alpha}\ddot{\Omega} - A = 0 \qquad (1)$$

where A and α are the constants of experience and Ω is an appropriate measurable quantity. The dot refers to differentiation with respect to time. Quantities that can be represented by Ω include strains for deforming alloys, metals, polymers, concrete, soil, rock, or ice. Fields of potential application of Eq. 1 include materials science, various branches of engineering, and the earth sciences. Although the question needs to be explored further, Eq. 1 may also apply (at least approximately) to predominantly rate-independent applications, such as some cases of fatigue (rate-independent repeated loading).

Additional relations may be deduced from Eq. 1, valid for several different groups of observables. Such equivalent cases include numerous independently discovered empirical or quasi-deterministic equations that describe time-deformation relations of creep to failure, and to a certain extent such cases provide validation for the basic proposition. The equation can also be used in the forecasting of specific new phenomena and in the solution of practical problems such as failure prediction. Such matters may be of importance to public safety; for example, at Vaiont, Italy, thousands died in a flood wave induced by the failure of a reservoir slope that could have been anticipated by Eq. 1 (*1*). Other potential applications include the failure of structural components, volcanic eruption forecasting, and the prediction of earthquakes (*2*).

Equation 1 is derived from experimental

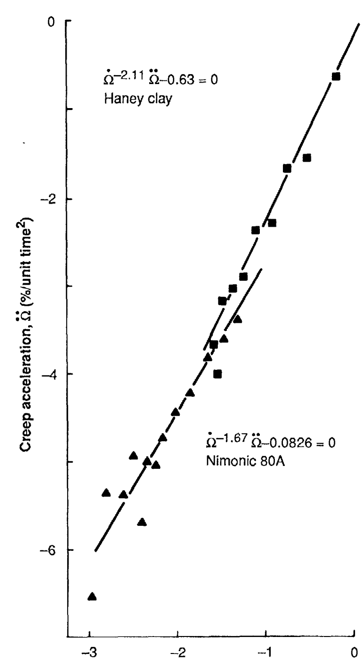

Fig. 1. The relation between creep acceleration ($\ddot{\Omega}$) and creep velocity ($\dot{\Omega}$) in terminal stages of creep of an alloy (Nimonic 80A) in tension and a soil (Haney clay) in compression (*5, 6*). Unit time is hours for Nimonic 80A and minutes for Haney clay.

College of Earth and Mineral Sciences, Pennsylvania State University, University Park, PA 16802.